scientific reports

Check for updates

OPEN

Experimental investigation of Al_2O_3 and CeO_2 nanoparticle additives in diesel-cottonseed biodiesel (CSOME) blends for performance and emission mitigation in a CI engine

Debas Dessie[1], Eyob Sisay Yeshanew[2]✉, Ramesh Babu Nallamothu[3] & Getachew Gashaw[4]

Diesel fuel is widely used, but environmental pollution and the limited availability of petroleum have raised concerns, prompting the search for cleaner alternatives. Biodiesel–diesel blends are considered eco-friendly options, and adding nanoparticles such as aluminum oxide (Al_2O_3) and cerium oxide (CeO_2) can further improve engine performance and reduce emissions. This study tested a single-cylinder, direct-injection diesel engine using pure diesel (B0), a 20% cottonseed biodiesel–diesel blend (B20), and B20 with 50 ppm Al_2O_3, 50 ppm CeO_2, and a combination of both nanoparticles. The biodiesel was prepared via transesterification and fuel properties, including density, viscosity, flash points, and calorific value, were measured. Engine tests showed that the combined Al_2O_3 and CeO_2 blend achieved the highest brake power of 3.56 kW at 3600 rpm and a brake torque of 8.6 N·m at 2400 rpm, while the lowest brake-specific fuel consumption of 0.258 kg/kW·h was recorded for this blend, indicating improved fuel efficiency. Emissions were significantly reduced: CO decreased to 6.7%, 11.2%, 9.7%, and 23.2%; CO_2 to 4.6%, 8.1%, 8.8%, and 14.8%; and hydrocarbon emissions to 5.9%, 10.2%, 8.1%, and 18.5% for B20, B20 + Al_2O_3, B20 + CeO_2, and B20 + Al_2O_3 + CeO_2, respectively. Oxygen concentration in the exhaust reached 17.97%, demonstrating more complete combustion. Overall, the B20 blend containing both Al_2O_3 and CeO_2 nanoparticles provided the best engine performance, fuel efficiency, and emission reduction, confirming its potential as a sustainable alternative to conventional diesel fuel.

Keywords Biodiesel, Emission, Engine performance, Nano particle, Transesterification

Abbreviations

Al	Aluminum
Al2O3	Aluminum oxide
ASTM	American standards for testing and materials
B0	Pure diesel
B20	80%Diesel and 20%biodiesel
B20 + 50ppmAl_2O_3	20% B_4C–80% SiC composite with 50 ppm Al_2O_3 added
B20 + 50 ppm CeO_2	20% B_4C–80% SiC composite with 50 ppm CeO_2 added

[1]Department of Mechanical Engineering, Ambo University, P.O. Box 19, Ambo, Ethiopia. [2]Department of Mechanical Engineering, Institute of Technology, University of Gondar, P.O. Box 196, Gondar, Ethiopia. [3]Department of Mechanical Engineering, School of Mechanical, Chemical and Materials Engineering, Adama Science and Technology University, P.O. Box 1888, Adama, Ethiopia. [4]Department of Mechanical Engineering, Aksum University, P.O. Box 1010, Aksum, Ethiopia. ✉email: eyobsisay17@gmail.com

B20 + 50ppmAl_2O_3 + 50 ppm CeO_2	20% B_4C + 80% SiC composite, with 50 ppm Al_2O_3 and 50 ppm CeO_2 added
B_4C	Boron Carbide
BET Analysis	Brunauer Emmett teller analysis
BN	Boron Nitride
BTE	Brake thermal efficiency
CH3OH	Methanol
CI	Compression Ignition
CO	Carbon monoxide
CO2	Carbon dioxide
CeO2	Cerium oxide
CNT	Carbon nanotubes
CSOME	Cottonseed methyl ether
CTAB	Cetyl trimethyl ammonium
DEE	Diethyl ether
DMC	Di-methyl carbonate
DSC	Differential scanning calorimetry
EGR	Exhaust gas recirculation
FAME	Fatty acid methyl esters
FFA	Free fatty acids
FTIR	Fourier Transform Infrared Spectroscopy
HC	Hydrogen carbide
Kg/kW.hr	Kilogram per kilowatt per hour
KOH	Potassium hydroxide
Nm	Newton meter
MWCNT	Multi-walled carbon nanotubes
NO	Nitric oxide
NOx	Nitrogen oxides
oC	Degree celicious
PDI	Polydispersity Index
PM	Particulate matter
ppm	Parts per million
rpm	Revolution per minute
s	Second
SCADA	Supervisory control and data acquisition
SEM	Scanning electron microscopy
SiC	Silicon carbide
SSA	Specific surface area
SOx	Sulfur oxides
TEM	Transmission electron microscopy
TGA	Thermogravimetric analysis
VI	Viscosity index
WCO	Waste cooking oil
XRD	X-ray diffraction

Petroleum-derived fuels have powered road transport for over a century; however, their finite reserves and increasingly stringent emission regulations have necessitated the development of cleaner and renewable energy sources[1]. Among these, biofuels, particularly biodiesel, offer a promising and sustainable alternative to conventional petroleum-based fuels. Biodiesel can be produced from agricultural feedstocks or waste oils, significantly reducing net greenhouse gas emissions through a closed-loop carbon dioxide (CO_2) cycle, and can be utilized in existing compression ignition (CI) engines without major modifications[2,3]. Biodiesel consists of mono-alkyl esters produced primarily via base-catalyzed transesterification of triglycerides (such as vegetable oils or animal fats) with short-chain alcohols like methanol. This process yields a fuel that meets ASTM D6751 or EN 14,214 standards and glycerol as a valuable by-product[4]. Owing to its inherent oxygen content, biodiesel promotes more complete combustion, leading to significant reductions in particulate matter (PM), carbon monoxide (CO), and unburned hydrocarbons (HC). Several studies have identified the oxygen mass fraction as a key factor contributing to PM reduction[5,6].

Beyond emission reduction, biodiesel offers additional advantages: it is sulphur-free, non-toxic, has a high flash point (> 100 °C), and biodegrades approximately four times faster than petroleum diesel, thereby reducing environmental risks associated with fuel spills[7]. Furthermore, life-cycle assessments have shown that biodiesel can achieve 50–90% lower net CO_2 emissions depending on the feedstock and production process. It also enhances fuel lubricity, extending engine component life, and supports rural economies by creating agricultural market opportunities[8,9]. Among the various biodiesel feedstocks, cottonseed oil methyl ester (CSOME) is particularly attractive because of its diesel-like physicochemical properties and its non-competitive relationship with food resources[10]. However, similar to other biodiesels, CSOME exhibits around 10% lower energy content, higher viscosity, and inferior cold-flow characteristics, which can negatively affect combustion efficiency and fuel atomization[11,12].

To overcome these limitations, the use of nano-additives such as aluminum oxide (Al_2O_3) and cerium oxide (CeO_2) has gained significant attention[13,14]. When dispersed in diesel or biodiesel blends at particle sizes below 100 nm, these nanoparticles provide large reactive surface areas, catalyze in-cylinder oxidation, enhance soot oxidation, release lattice oxygen (oxygen buffering), and reduce ignition delay[15,16]. Prior to blending, the nanoparticles were characterized to confirm their morphology, size, and chemical composition. Scanning Electron Microscopy (SEM) was employed to examine particle shape, X-ray Diffraction (XRD) to identify crystalline phases, Fourier Transform Infrared Spectroscopy (FTIR) to detect functional groups, and Transmission Electron Microscopy (TEM) to analyze size distribution[17]. An effective additive must remain stably suspended in the fuel, resist shear forces, prevent abrasive wear, and deliver measurable performance and emission benefits without producing harmful by-products[18,19]. Previous research has demonstrated that CSOME-based blends reduce smoke emissions and maintain torque levels comparable to diesel, despite a 3–5% reduction in torque due to lower heating values[20,21]. This study therefore aims to comprehensively evaluate the synergistic effects of a dual-nanoparticle additive formulation (50 ppm Al_2O_3 + 50 ppm CeO_2) in B20 cottonseed oil biodiesel–diesel blends on engine performance and emissions. The investigation focuses on key parameters, including brake power (BP), brake torque (Tb), brake-specific fuel consumption (BSFC), and the emissions of CO, CO_2, HC, and O_2 across the full engine operating range (1154–3840 rpm). To ensure accurate and reproducible results, optimized ultrasonication protocols were applied to ensure uniform nanoparticle dispersion and mixture homogeneity[22–24].

Literature review

Biodiesel derived from non-edible feedstocks such as Jatropha, Karanja, and cottonseed has garnered considerable attention as a sustainable alternative fuel for compression ignition (CI) engines. These biodiesels generally reduce emissions of carbon monoxide (CO), hydrocarbons (HC), and smoke opacity by 10–60%, owing to their inherent oxygen content that promotes more complete combustion. However, they often induce a slight increase in nitrogen oxides (NO_x) emissions, typically around 2–4%, attributed to elevated in-cylinder temperatures during combustion[25,26]. Among the non-edible feedstocks, cottonseed oil methyl ester (CSOME) stands out due to its diesel-like properties and the advantage of not competing with food resources, making it a desirable option[27]. Nevertheless, CSOME's approximately 10% lower energy density and higher viscosity impair fuel atomization and combustion efficiency, leading to a 3–5% reduction in torque and brake thermal efficiency (BTE) compared to conventional diesel[28]. Although the emission benefits of cottonseed oil methyl ester (CSOME) are well-documented, optimizing its performance with nano-additives under varying engine loads remains an area requiring further research[29].

Diesel engines remain a primary power source, but environmental concerns and petroleum depletion have driven research toward sustainable alternatives. Biodiesel–diesel blends are widely studied for their eco-friendly properties, with additives and predictive models enhancing combustion and reducing emission. Hydrogen-assisted blends have been shown to improve flame propagation and fuel oxidation, leading to lower emissions[30]. Similarly, machine learning predictions for nanoparticle-enhanced pongamia biodiesel demonstrated up to 9.8% higher brake thermal efficiency (BTE) and 18.7% lower brake-specific fuel consumption (BSFC) compared to standard B20 blends[31]. These studies highlight the potential of advanced additives and data-driven strategies to optimize engine performance and reduce environmental impact. Collectively, they provide a strong foundation for ongoing research into sustainable and efficient diesel fuel technologies. Regarding biodiesel production, base-catalysed transesterification continues to be the predominant method for CSOME synthesis, typically employing methanol with sodium or potassium hydroxide catalysts at molar ratios of 6:1 to 10:1 and reaction temperatures between 55 and 65 °C, yielding conversion efficiencies exceeding 95%[32]. Although acid pretreatment and supercritical transesterification techniques enable the use of feedstocks with high free fatty acid content, their industrial scalability is limited due to high cost and process complexity[33]. Recent research has focused on improving catalyst recovery and valorising waste oils to enhance sustainability[33,34]; however, integrating nano-additives during biodiesel production, especially for CSOME, remains an underexplored area.

Nano-additives have emerged as promising agents to improve emission profiles and engine performance synergistically. Cerium oxide (CeO_2), for example, functions as an oxygen buffer and catalyst, reducing CO and HC emissions by up to 80% and 60%, respectively, while also lowering NO_x emissions by approximately 45% through catalytic oxidation processes[35]. Alumina (Al_2O_3) nanoparticles enhance fuel–air mixing via micro-explosive combustion effects, resulting in NO_x reductions of around 35% when blended with CSOME fuels[36]. Specifically, CeO_2 addition to CSOME blends has been reported to decrease smoke emissions by 27% and reduce brake-specific fuel consumption (BSFC) by 9.3% at 2400 rpm[37]. Conversely, Al_2O_3 at 50 ppm concentration in B20 cottonseed biodiesel blends improved BTE by 8.5% but showed limited control over HC and CO emissions[38]. Hybrid nano-additive systems, such as CeO_2 combined with multi-walled carbon nanotubes (MWCNTs), have achieved soot reductions nearing 48%, even though with increased complexity and cost[39]. Although many studies have shown that nano-additives like CeO_2 and Al_2O_3 can improve biodiesel performance, there is very little research on how they work together in cottonseed biodiesel (CSOME). Studies

Item	Specification	Al_2O_3	CeO_2
Manufacturer		NRL, USA	NRL, USA
Purity		99.9%	99.9%
Average particle size		30–50 nm	20–30 nm
Specific surface area (SSA)		130–140 m^2/g	40–45 m^2/g
Color		White	Light Yellow
Density		3.97 g/cm^3	6.5 g/cm^3
SEM (scanning electron microscopy)	Morphology & Particle Shape	Nearly spherical particles with uniform distribution	Slightly agglomerated spherical nanoparticles
FTIR (fourier transform infrared spectroscopy)	Functional Groups	Strong Al–O stretching vibration at ~ 540–570 cm^{-1}	Characteristic Ce–O stretching band at ~ 460–480 cm^{-1}
XRD (X-ray diffraction)	Crystalline Structure	Peaks correspond to γ–Al_2O_3 phase, confirming high crystallinity	Diffraction peaks indicate cubic fluorite structure of CeO_2
Zeta potential	Surface Charge & Stability	Typically + 35 to + 40 mV (stable dispersion)	Typically + 30 to + 35 mV (moderate stability)
BET analysis	Surface Area Verification	Confirms high SSA due to Nano-size range	Consistent with moderate SSA values

Table 1. Nanoparticle Specifications.

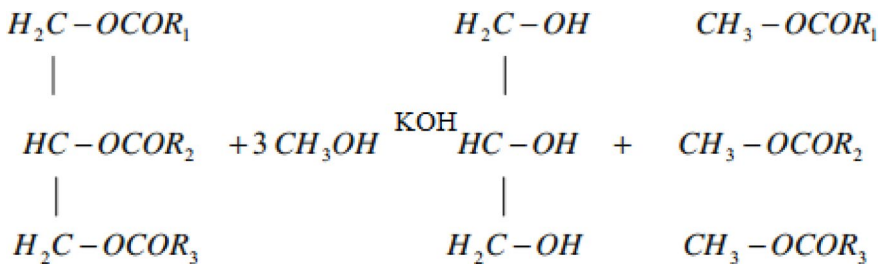

Fig. 1. Transesterification reactions with methanol[41,42].

using only one additive have shown drawbacks—for example, CeO_2 can increase NOx emissions, while Al_2O_3 may not reduce hydrocarbons (HC) or carbon monoxide (CO) effectively. Moreover, there has been limited investigation into the combined effects of Al_2O_3 and CeO_2 in CSOME blends at concentrations between 50 and 100 ppm, inconsistent nanoparticle dispersion techniques affecting reproducibility, and scarce data on the long-term impacts of nano-additives on engine wear and durability[40]. This study fills these gaps by evaluating a B20 CSOME blend containing individual nanoparticles (50 ppm Al_2O_3 or 50 ppm CeO_2) and a hybrid combination (50 ppm Al_2O_3 + 50 ppm CeO_2) to determine whether the hybrid additive can integrate the advantages of both nanoparticles to improve engine performance and lower emissions.

Materials and methods

The materials used in this study included a range of feedstocks, chemicals, nano-additives, and laboratory equipment essential for biodiesel production and engine performance testing. Cottonseed oil (*Gossypium arboreum L.*), belonging to the Malvaceae family, was sourced from Addis Mojo Oil Factory (Ethiopia) and selected as the primary feedstock owing to its high triglyceride content, wide availability as an agricultural byproduct, and favourable properties compared with other vegetable oils such as soybean and palm oil. Commercial petroleum diesel fuel was obtained from Oil Libya, Adama, Ethiopia, and used for blending with the cottonseed oil methyl ester (CSOME).

Biodiesel production process

For the transesterification process, analytical-grade methanol (99.8% purity) was used as the alcohol, sodium hydroxide (NaOH) was the base catalyst, and distilled water was used for washing and purification. Al_2O_3 and CeO_2 nanoparticles, obtained with 99.9% purity, were of nanoscale particle sizes 30–50 nm for Al_2O_3 and 20–30 nm for CeO_2, with favourable density and surface area characteristics. Their specifications are summarized in Table 1.

The cottonseed oil methyl ester (CSOME) was produced through an alkali-catalyzed transesterification process. In this process, vegetable oils or animal fats react with alcohol (such as methanol) in the presence of a catalyst(NaOH) to produce Fatty Acid Methyl Esters (FAME), commonly known as biodiesel, with glycerin as a by-product, as illustrated in Fig. 1. The resulting FAME mixture is then purified to remove contaminants such as catalyst residues, methanol, and water.

$$RCOO\prime + R\prime\prime OHR\prime OH + RCOOR\prime\prime$$

RCOOR' indicates an ester, R"OH an alcohol, R'OH another alcohol (glycerol),
RCOOR" is an ester mixture and acts as a catalyst.

The detailed production steps are described in the following sections. The procedure began with a pre-treatment step in which the cottonseed oil was titrated to determine its free fatty acid (FFA) content, measured at 1.72 mg KOH/g. This value confirmed the oil's suitability for a single-step transesterification process without acid pre-treatment[43,44]. For the transesterification reaction, 500 mL of cottonseed oil was mixed with the methoxide solution, prepared by dissolving 5 g of sodium hydroxide (NaOH) in 100 mL of methanol. The mixture was stirred at 1000 rpm and maintained at 60 °C for 60 min to ensure complete reaction. After the reaction, the mixture was allowed to settle for 24 h to facilitate phase separation, during which glycerol formed at the bottom and was separated from the upper CSOME layer, as illustrated in Fig. 2.

Purification of the reaction products

After separating glycerin from the reaction mixture, the produced fatty acid methyl esters (FAME) still contained impurities such as residual methanol, NaOH, and glycerin. These contaminants negatively affect biodiesel quality by increasing the cloud and pour points and lowering the flash point[45,46]. Therefore, a purification process was essential to meet the required standards, such as ASTM D6751 and EN 14214[47]. The biodiesel was purified by washing with warm distilled water at 60 °C to remove residual impurities. The cottonseed oil methyl ester (CSOME) was placed in a separating funnel, and half the volume of heated water was added to wash the ester. The mixture was allowed to settle, and the contaminated water was removed by opening the funnel's valve. This process was repeated five times until the wash water appeared clear. The washing continued for 24 h while maintaining the temperature at 60 °C to ensure thorough removal of contaminants. A high amount of soap and impurities was observed during the first wash, settling at the bottom of the separator. Finally, the purified CSOME was dried by heating it to 130 °C to eliminate any remaining moisture content, as illustrated in Fig. 3.

Preparation of diesel–biodiesel blends and nanoparticles

B20 fuel, consisting of 20% cottonseed oil methyl ester (COME) biodiesel and 80% petro-diesel, was used as the base blend for performance testing. To enhance fuel characteristics, aluminum oxide (Al_2O_3) and cerium oxide (CeO_2) nanoparticles were incorporated into the B20 blend at a concentration of 50 ppm each. The nanoparticles were dispersed using an ultrasonic cleaner operating at 120 W and 40 kHz for 40 min, with cetyl trimethyl ammonium bromide (CTAB) added as a surfactant to improve nanoparticle stability and dispersion. Three

Fig. 2. Transesterification process flow steps: (1) Oil preheating, (2) Methoxide preparation, (3) Reaction, (4) Glycerol separation, (5) Biodiesel washing and drying.

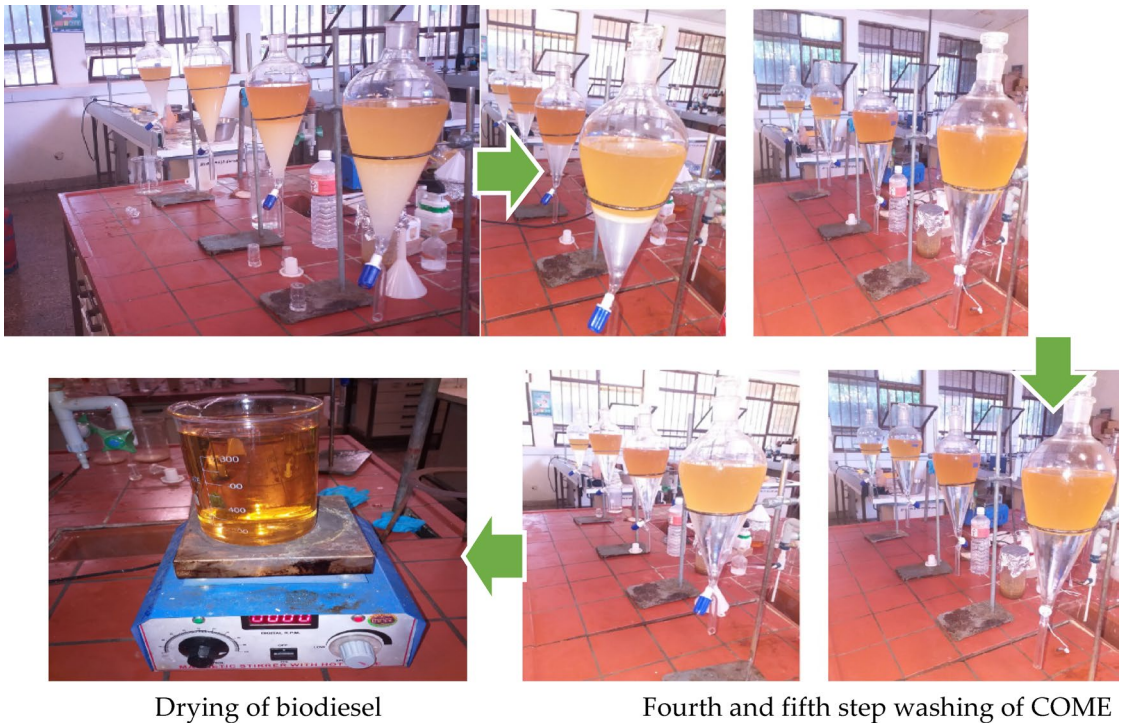

Fig. 3. Cleaning process.

nano-fuel blends were prepared: B20A50 (B20 with 50 ppm Al_2O_3), B20C50 (B20 with 50 ppm CeO_2), and B20A50C50 (B20 with both 50 ppm Al_2O_3 and 50 ppm CeO_2). The blending process used standard laboratory equipment, including Beakers, an Ultrasonic cleaner, a Digital balance, a Hot plate with magnetic stirrer, Cerium oxide nano particle, Aluminum oxide nanoparticles, Cetyle trimethyl ammonium bromide (CTAB), petrodiesel, and prepared cottonseed oil biodiesel[40], as shown in Fig. 4.

Fuel samples were prepared through a systematic procedure. First, the B20 blend was prepared by mixing 800 ml of diesel with 200 ml of biodiesel (20% by volume) in a 1-L bottle, followed by vigorous shaking for at least two minutes to ensure uniform blending. For nanoparticle dispersion, 1000 ml of the B20 blend was measured into a beaker. Specific nanoparticle-surfactant combinations were added: 0.05 g Al_2O_3 with 0.05 g CTAB for B20 + Al_2O_3 (50 ppm), 0.05 g CeO_2 with 0.05 g CTAB for B20 + CeO_2 (50 ppm), and a combination of 0.05 g Al_2O_3, 0.05 g CeO_2, and 0.05 g CTAB each for B20 + Al_2O_3 + CeO_2 (50 ppm each). Each mixture was stirred for at least 15 min and then poured into the remaining 900 ml of the respective B20 fuel bottle. To ensure thorough homogenization, all fuel blends (B20 and nanoparticle-modified B20) were processed in an ultrasonic cleaner at 40 kHz and 40 °C for 40 min, as shown in Fig. 5. Finally, the cleaning process switches off the ultrasonic cleaner using the "power on/off" key and disconnects the power supply. The final prepared fuel samples, showing the five main blends and their corresponding similar products, are shown in Fig. 6.

Determination of fuel properties

The physicochemical properties of B20 and its nanoparticle-enriched blends were evaluated following ASTM standards[18], and the results are summarized in Table 2. All tested fuels complied with the required standards for diesel–biodiesel blends. Density values (0.8435–0.8447 g/ml) were consistent with diesel limits (0.82–0.86), ensuring reliable injection performance. The flash points of the blends (85–87 °C) were lower than neat biodiesel (185 °C) but well above the diesel standard (ASTM D975, ≥ 52 °C), confirming safe handling and storage [ASTM D975; ASTM D6751][48,49]. The cloud point remained nearly constant at ≈2 °C, within the acceptable biodiesel range (− 3 to 12 °C). Importantly, the kinematic viscosity decreased with nanoparticle addition, from 4.428 cSt (B20) to 3.890 cSt (B20 + CeO_2), improving flow and atomization while staying within ASTM limits (1.9–6.0 cSt)[50,51]. The calorific value consistently increased with the addition of nanoparticles. While the absolute gains are relatively small, statistical analysis confirmed that the increases for the B20 + Al_2O_3 ($p < 0.05$), B20 + CeO_2 ($p < 0.05$), and B20 + Al_2O_3 + CeO_2 ($p < 0.01$) blends are statistically significant compared to the base B20 fuel, indicating that these improvements are genuine and exceed the measurement uncertainty. Overall, the ternary blend (B20 + Al_2O_3 + CeO_2) showed the most balanced improvement in fuel properties, making it the most suitable candidate for diesel engine applications[52–54].

Experimental setup and procedure

Engine performance and emission characteristics were evaluated using the TBMC3-02 computer-controlled test bench, which houses a single-cylinder, four-stroke, air-cooled diesel engine manufactured by Edibon, as detailed in Table 3.

a) Ultrasonic cleaner b) Digital balance c) Hot plate with magnetic stirrer

a) CTAB b) Aluminum oxide nanoparticle c) Cerium oxide nanoparticle

Fig. 4. The equipment and materials used for diesel–biodiesel-nanoparticle blending.

Fig. 5. Ultrasonic cleaning process.

The TBMC3-02 test bench, comprised six core components: (1) Diesel engine, (2) Asynchronous motor dynamometer for torque/power measurement and load application, (3) fuel tank, (4) SCADA control system with real-time data acquisition, (5) Computer, and (6) Exhaust gas analyzer for monitoring emissions, as shown in Fig. 7. The engine performance and emission tests were conducted under steady-state conditions. All measurements were taken at a constant full load (100% of maximum torque) while the engine speed was varied. The specific speeds investigated were 1154, 1250, 1500, 2000, 2400, 3000, 3600, and 3840 rpm. At each stabilized speed and load point, data for performance parameters and emissions were recorded.

Fig. 6. Prepared fuel samples for the test.

Property	Test method	ASTM D6751 (B100)	B20	B20+Al_2O_3	B20+CeO_2	B20+Al_2O_3+CeO_2
Density @20 °C (g/ml)	D4052	0.86–0.90	0.8435 ± 0.0010	0.8442 ± 0.0009	0.8445 ± 0.0011	0.8447 ± 0.0010
Flash Point (°C)	D93	≥130	86 ± 1.5	87 ± 1.3	87 ± 1.6	85 ± 1.4
Cloud Point (°C)	D2500	−3 to 12	2 ± 0.5	2 ± 0.5	2 ± 0.5	2 ± 0.5
Viscosity @40 °C (cSt)	D562	1.9–6.0	4.428 ± 0.050	4.216 ± 0.045	3.890 ± 0.055	4.009 ± 0.048
Calorific Value (MJ/kg)	D240	37–42	39.45 ± 0.08	39.61 ± 0.07	39.64 ± 0.09	39.86 ± 0.07

Table 2. Physicochemical properties of prepared fuels[51].

Engine Manufacture	Edibon
Type of engine	Compression ignition
Fuel	Diesel
Number of cylinders	1
Number of strokes	Four
Type of air intake	naturally aspirated
Type of cooling	Air
Start	Computer-controlled / manual
Compression ratio	21:1
Maximum power	4.2HP/3.13kw @ 3600 rpm
Cylinder bore	69 mm
Stroke	60 mm
Swept volume (displacement)	224 cm^3
Injection timing	23° before Top Dead Centre (BTDC)
Injection pressure	200 bar
Valve mechanism	Overhead valve (OHV)
Governing type	Centrifugal mechanical governor
Exhaust gas analyzer	Integrated with test setup

Table 3. Specification of TBM3-02 test bench for single-cylinder diesel engine[55].

The test bench was equipped with an integrated Supervisory Control and Data Acquisition (SCADA) system, EDIBON SCADA Software (ESS), Version 2.1 (https://www.edibon.com/en/computer-controlled-test-bench-for-2-2-kw-engines), which enabled real-time monitoring, control, and data collection. The SCADA-based control and monitoring system comprised five core components: (1) Main software operations, (2) Sensor displays, (3) Actuator controls, (4) Channel selection and other plot parameters, and (5) Real-time graphics display, as shown in Fig. 8.

Test fuels

The experiments were then conducted included five samples: pure petro-diesel (B0), a baseline biodiesel blend (B20: 20% cottonseed oil methyl ester (CSOME) + 80% diesel), and three nanoparticle-enhanced variants,

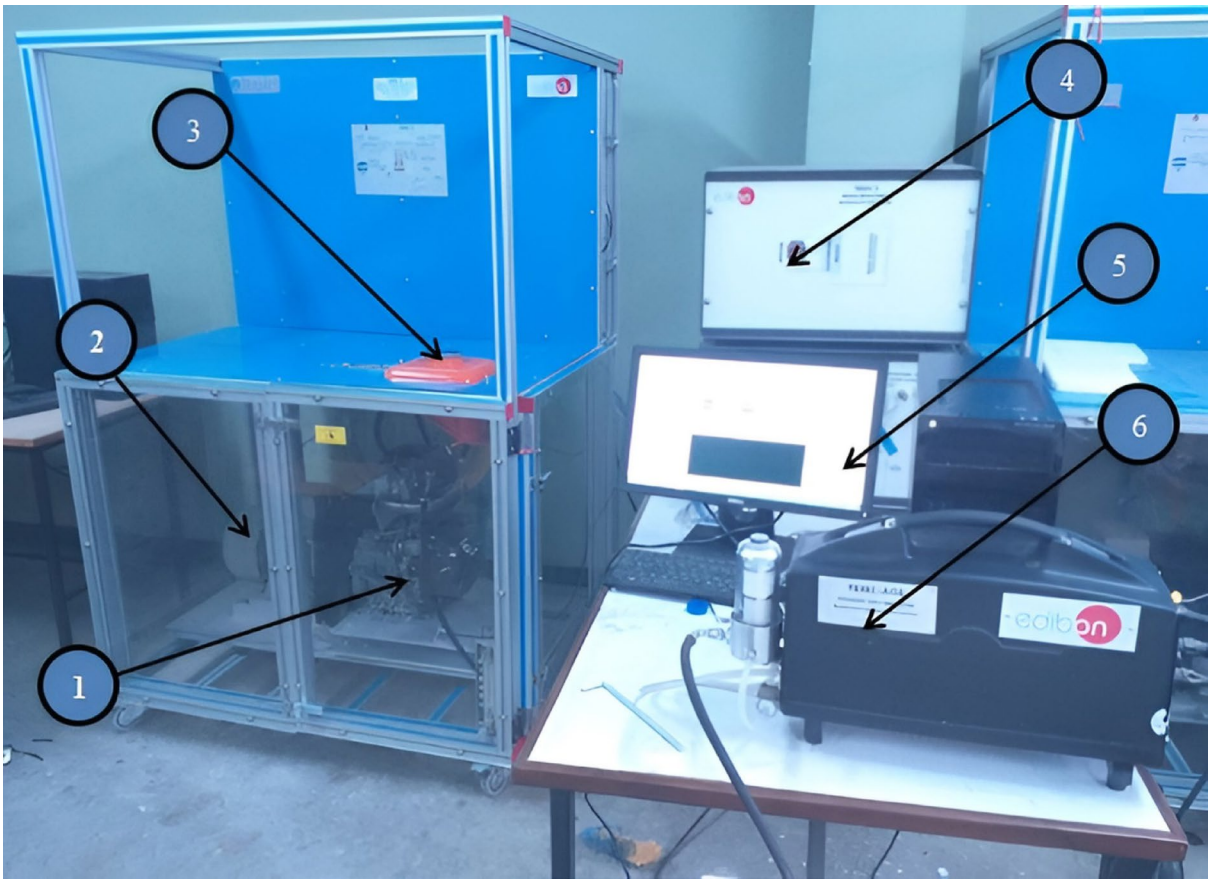

Fig. 7. Experimental setup of TBM3-02 test bench for single-cylinder diesel engine.

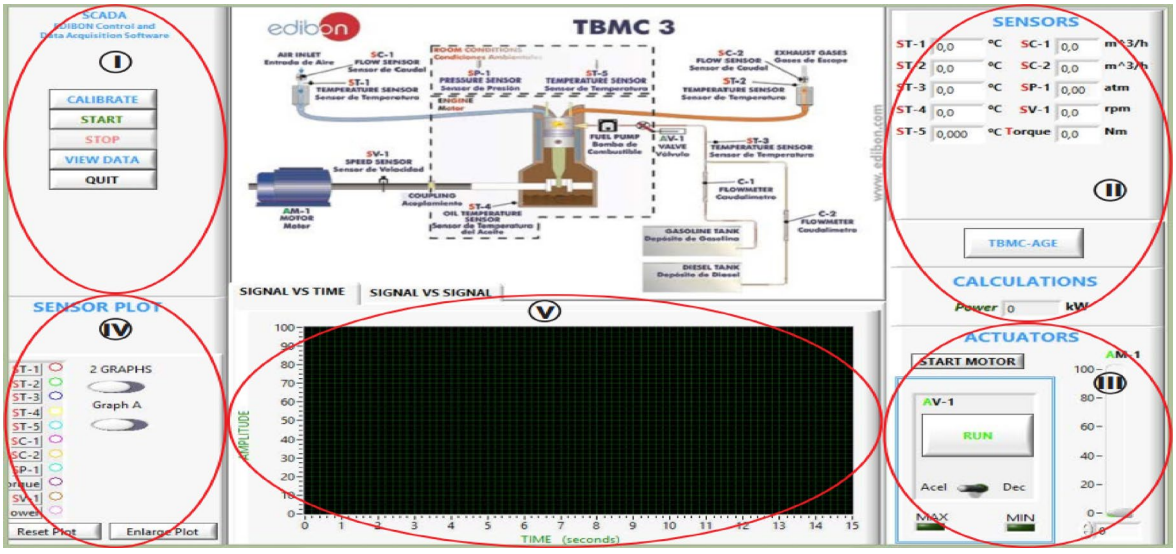

Fig. 8. SCADA main screen.

B20 + 50 ppm Al_2O_3 (B20A50), B20 + 50 ppm CeO_2 (B20C50), and B20 + 50 ppm Al_2O_3 + 50 ppm CeO_2 (B20A50C50).

Preparation
Before testing, the lubricating oil level was checked, the fuel tank was filled with the respective sample, and electrical connections were established. The SCADA software was then initialized, and the engine was allowed to idle for 10 min to reach thermal stabilization. The full experimental setup is illustrated in Fig. 9.

Performance testing

Performance testing was done by gradually applying incremental loads using the dynamometer while monitoring engine parameters through SCADA (Fig. 3.23). At each load step, brake power (BP), brake torque (Tb), mass fuel consumption (mf), and brake-specific fuel consumption (BSFC) were calculated using Equations:

Brake power (BP)
Is the engine's usable output at the crankshaft, measured with a power absorption device. It is calculated using the equation:

$$T_b = \frac{WL \times 2\pi N}{60} (W) \tag{1}$$

where; P_b = Brake power in W, W_L = torque in N·m, and N = Engine speed in rpm.

BrakeTorque(Tb)
Represents the usable torque available at the engine's flywheel, was measured for each test fuel across various engine speeds using the TBMC-3 test bench.

$$T_b = \frac{60P_b}{2\pi N} (N.m) \tag{2}$$

where; T_b = engine brake torque in N.m, P_b = engine brake power in kW, and N = engine speed in rpm.

Mass fuel consumption (mf)
Was measured by recording the time taken to consume a known fuel volume. The mass of fuel was then calculated by multiplying the volume by fuel density, using the following equation:

$$m_f = v_f x_f g/s \tag{3}$$

where; v_f = the volume flow rate of the fuel in ml/min, and = density of fuel in g/ml.

Brake-specific fuel consumption (BSFC)
Is the fuel consumed per hour per unit of brake power. It was determined at various operating conditions using the following equation:

$$BSFC = \frac{m_f * 3600}{P_b} kg/kW.hr \tag{4}$$

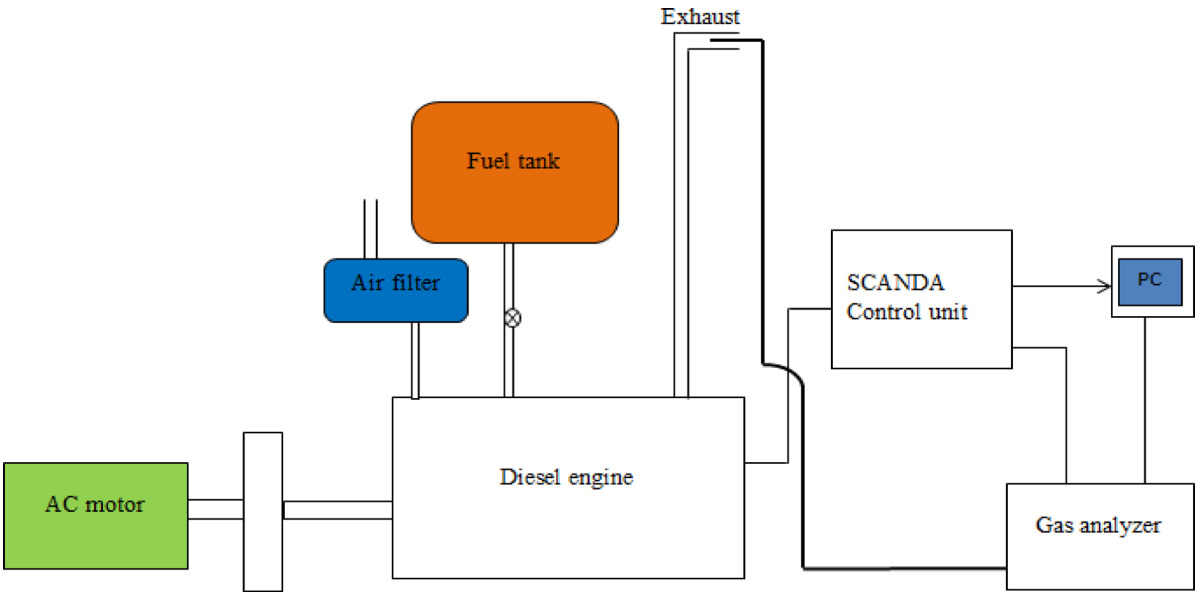

Fig. 9. Diagrammatic experimental setup.

Where, m_f is the mass of fuel consumed in kg/s, and BP is the brake power in kW.

Emission testing

Once the engine achieved thermal stability, the same load sequence was applied while maintaining constant speed at each load level. The TBMC_AGE analyzer continuously measured the exhaust gas concentrations of CO, CO_2, HC, and O_2, and all data were logged through SCADA. This procedure was repeated for all fuel samples, B0, B20, B20 + 50 ppm Al_2O_3, B20 + 50 ppm CeO_2, and B20 + 50 ppm Al_2O_3 + 50 ppm CeO_2, under different loads and speeds to allow consistent and comparable evaluation of engine emissions.

Result and discussion

The study examined the effects of aluminum oxide (Al_2O_3) and cerium oxide (CeO_2) nanoparticles on the emission and performance characteristics of a compression ignition (CI) engine. The nanoparticles improve fuel atomization and evaporation, generating finer fuel droplets and better air–fuel mixing, which ensures uniform and stable combustion. Their catalytic activity accelerates oxidation reactions, leading to the complete conversion of carbon monoxide (CO) and unburned hydrocarbons (HC) into carbon dioxide (CO_2), while also increasing the heat release rate and reducing ignition delay, thereby improving thermal efficiency. Furthermore, CeO_2 acts as an oxygen carrier, storing and releasing oxygen during combustion to maintain an optimal oxygen balance in the cylinder, facilitating more complete fuel oxidation and minimizing harmful emissions. Test fuels included petroleum diesel (B0), B20 biodiesel derived from cottonseed oil, and nanoparticle-enhanced B20 blends. Emission analysis considered carbon monoxide (CO), carbon dioxide (CO_2), hydrocarbons (HC), and oxygen (O_2) concentrations, while performance evaluation focused on brake power (BP), brake torque (BT), and brake specific fuel consumption (BSFC).

Performance characteristics

Brake power

Brake power exhibited a clear increasing trend with engine speed for all tested fuel samples, attaining a peak value at 3600 rpm before experiencing a slight decline at higher speeds, as illustrated in Fig. 10. Among the fuels tested, the B20 biodiesel blend enhanced with a combination of 50 ppm Al_2O_3 and 50 ppm CeO_2 nanoparticles demonstrated the highest brake power, reaching 3.56 kW at 3600 rpm. This value represents a significant improvement compared to conventional diesel (B0), which delivered a maximum brake power of 3.01 kW, and the unmodified B20 blend, which achieved 2.89 kW at the same engine speed. The observed enhancement in brake power can be attributed to the improved combustion characteristics provided by the synergistic effect of the Al_2O_3 and CeO_2 nanoparticles, which promote better atomization, faster oxidation, and more complete fuel burning under high-speed operating conditions.

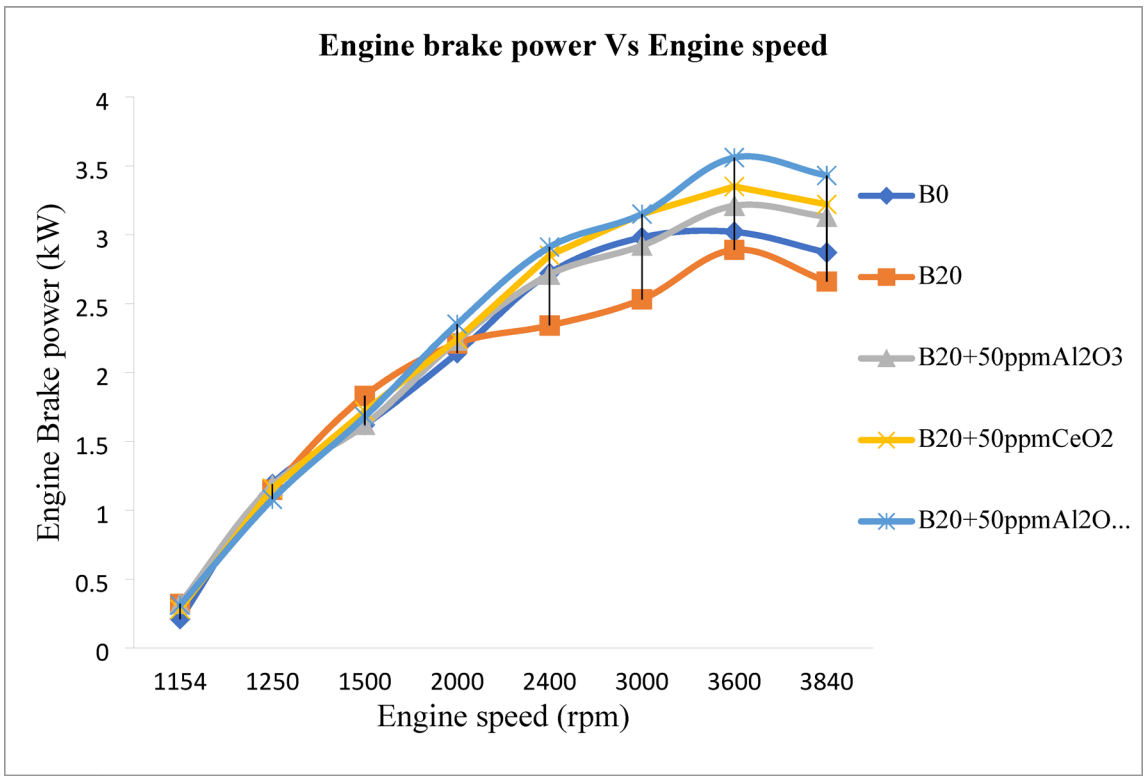

Fig. 10. Brake power at different engine speeds.

Brake torque

The engine brake torque exhibited a distinct variation with engine speed for all tested fuels, initially increasing as the speed rose, reaching a maximum at 2400 rpm, and subsequently decreasing at higher speeds, as illustrated in Fig. 11. The peak torque values were observed consistently at 2400 rpm across all fuel types, indicating the engine's optimal torque-producing condition. Specifically, conventional diesel (B0) achieved a maximum torque of 8.5 Nm, while the unmodified B20 blend produced 8.1 Nm. The addition of nanoparticles enhanced the torque values, with B20 + 50 ppm Al_2O_3 reaching 8.2 Nm and B20 + 50 ppm CeO_2 achieving 8.4 Nm. The highest torque was recorded for the B20 blend containing a combination of 50 ppm Al_2O_3 and 50 ppm CeO_2, which reached 8.6 Nm at 2400 rpm. This improvement in torque can be attributed to the catalytic effect of the metal oxide nanoparticles, which promote more efficient combustion, improve fuel–air mixing, and enhance energy conversion within the cylinder, particularly at mid-range engine speeds.

Brake-specific fuel consumption (BSFC)

Brake specific fuel consumption (BSFC) demonstrated a consistent decreasing trend with increasing engine speed for all tested fuels. This behavior is attributed to the engine generating higher power outputs at elevated speeds without a proportional increase in fuel consumption, reflecting improved energy utilization[56]. Among the fuels examined, the B20 biodiesel blend exhibited the highest BSFC values, primarily due to its lower calorific value and higher density compared to conventional diesel, which necessitated a greater fuel mass to achieve the same power output. The incorporation of metal oxide nanoparticles, specifically Al_2O_3 and CeO_2, enhanced the combustion characteristics of the B20 blend, leading to a notable reduction in BSFC across the tested speed range. The most significant improvement was observed for the B20 blend containing a combination of 50 ppm Al_2O_3 and 50 ppm CeO_2, which achieved the lowest BSFC of 0.258 kg/kW.h at 3840 rpm. This reduction indicates that the nanoparticles facilitated more complete and efficient fuel oxidation, improved atomization, and enhanced thermal energy conversion within the combustion chamber, thereby allowing the engine to deliver higher power output with lower fuel consumption, as illustrated in Fig. 12.

Emission characteristics

CO emission

Carbon monoxide (CO) emissions were significantly reduced with the incorporation of nanoparticles into the B20 biodiesel blend. Among the tested fuels, the B20 + Al_2O_3 + CeO_2 blend exhibited the lowest CO emissions, measuring 0.075%, which corresponds to a 23.2% reduction relative to conventional diesel (B0). This substantial decrease can be attributed to the catalytic oxidation properties of Al_2O_3 and CeO_2 nanoparticles, which enhance the conversion of carbon monoxide (CO) to carbon dioxide (CO_2) during combustion, thereby promoting more complete fuel oxidation[57]. In terms of average emission reductions across the tested fuels, the unmodified B20

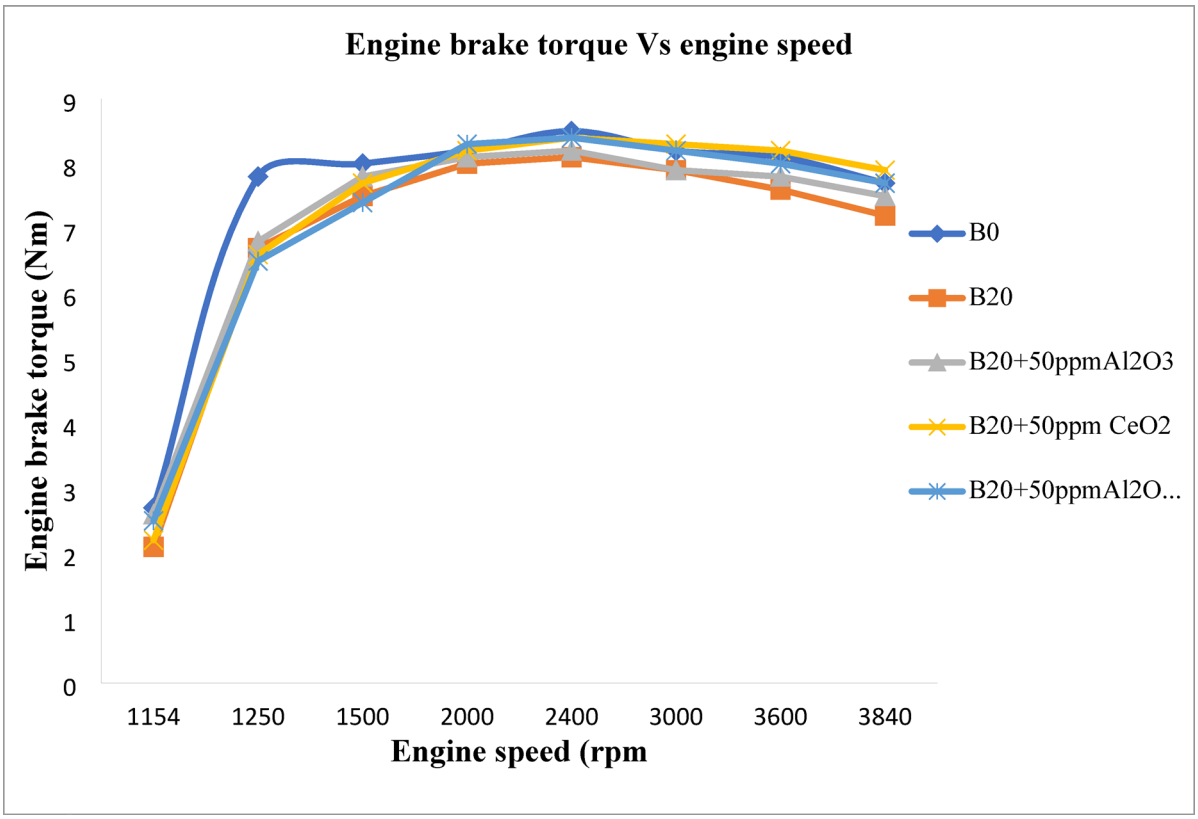

Fig. 11. Engine speed VS brake power.

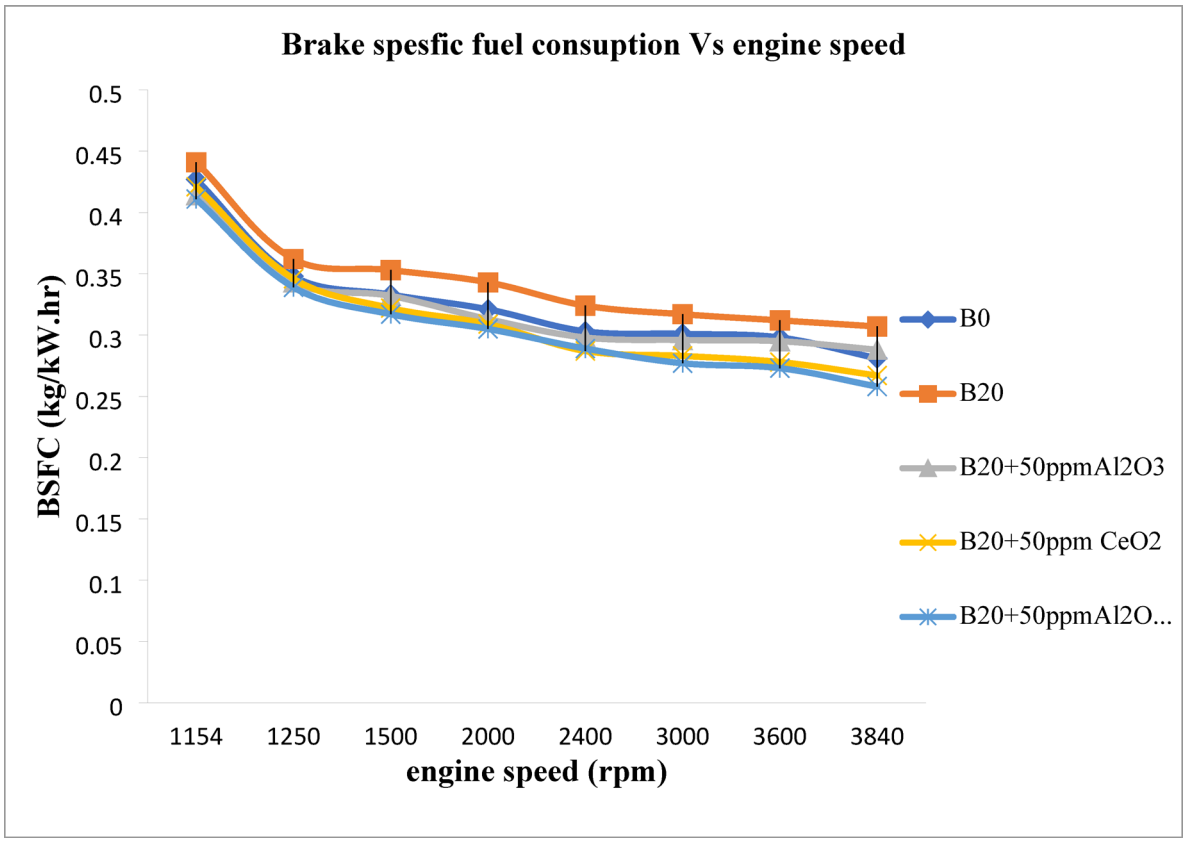

Fig. 12. The variation of brake-specific fuel consumption with engine speed.

blend achieved a 6.7% decrease, B20 + Al_2O_3 reduced CO emissions by 11.2%, B20 + CeO_2 by 9.7%, and the combined B20 + Al_2O_3 + CeO_2 blend attained the highest reduction of 23.2%, as illustrated in Fig. 13. These results highlight the synergistic effect of the two nanoparticles, which not only improve combustion efficiency but also contribute to lower pollutant formation, demonstrating their effectiveness in mitigating CO emissions from biodiesel–diesel blends.

CO_2 emission

Carbon dioxide (CO_2) emissions also decreased with the addition of nanoparticles to the B20 biodiesel blend. The B20 + Al_2O_3 + CeO_2 combination exhibited the lowest recorded CO_2 concentration of 2.04% at 1154 rpm. In general, biodiesel blends produced lower CO_2 emissions than conventional diesel (B0), primarily due to their lower carbon-to-hydrogen ratio, which results in reduced carbon content per unit of fuel[58]. At 1554 rpm, the measured CO_2 emissions were 2.87% for B0, 2.64% for B20, 2.72% for B20 + Al_2O_3, 2.51% for B20 + CeO_2, and 2.51% for B20 + Al_2O_3 + CeO_2, as illustrated in Fig. 14. When averaged across the tested speed range, the reductions relative to B0 were 4.6% for B20, 8.1% for B20 + Al_2O_3, 8.8% for B20 + CeO_2, and 14.8% for the combined B20 + Al_2O_3 + CeO_2 blend. The observed decrease in CO_2 emissions can be attributed to the enhanced combustion efficiency provided by the nanoparticles, which promote more complete oxidation of the fuel and reduce the formation of excess carbon-containing exhaust gases. These results indicate that the synergistic effect of Al_2O_3 and CeO_2 nanoparticles not only improves engine performance but also contributes to mitigating greenhouse gas emissions from biodiesel–diesel blends.

Hydrocarbon (HC) emission

Hydrocarbon (HC) emissions were significantly reduced with the addition of nanoparticles to the B20 biodiesel blend. Among the fuels tested, the B20 + Al_2O_3 + CeO_2 combination exhibited the lowest HC emissions, measuring 15 ppm at 3840 rpm. Elevated HC emissions are typically associated with the presence of fuel-rich zones within the combustion chamber and incomplete combustion processes[59]. The experimental results demonstrated that all cottonseed biodiesel blends, including B20, B20 + Al_2O_3, B20 + CeO_2, and B20 + Al_2O_3 + CeO_2, produced lower HC emissions compared to conventional diesel (B0), as depicted in Fig. 15. The reduction in HC emissions can be attributed to the catalytic and thermal effects of Al_2O_3 and CeO_2 nanoparticles, which enhance fuel atomization, improve air–fuel mixing, accelerate flame propagation, and promote more complete combustion. Consequently, the use of these nanoparticles not only improves engine performance but also effectively mitigates unburned hydrocarbon emissions, highlighting their potential for cleaner and more efficient operation of biodiesel–diesel blends.

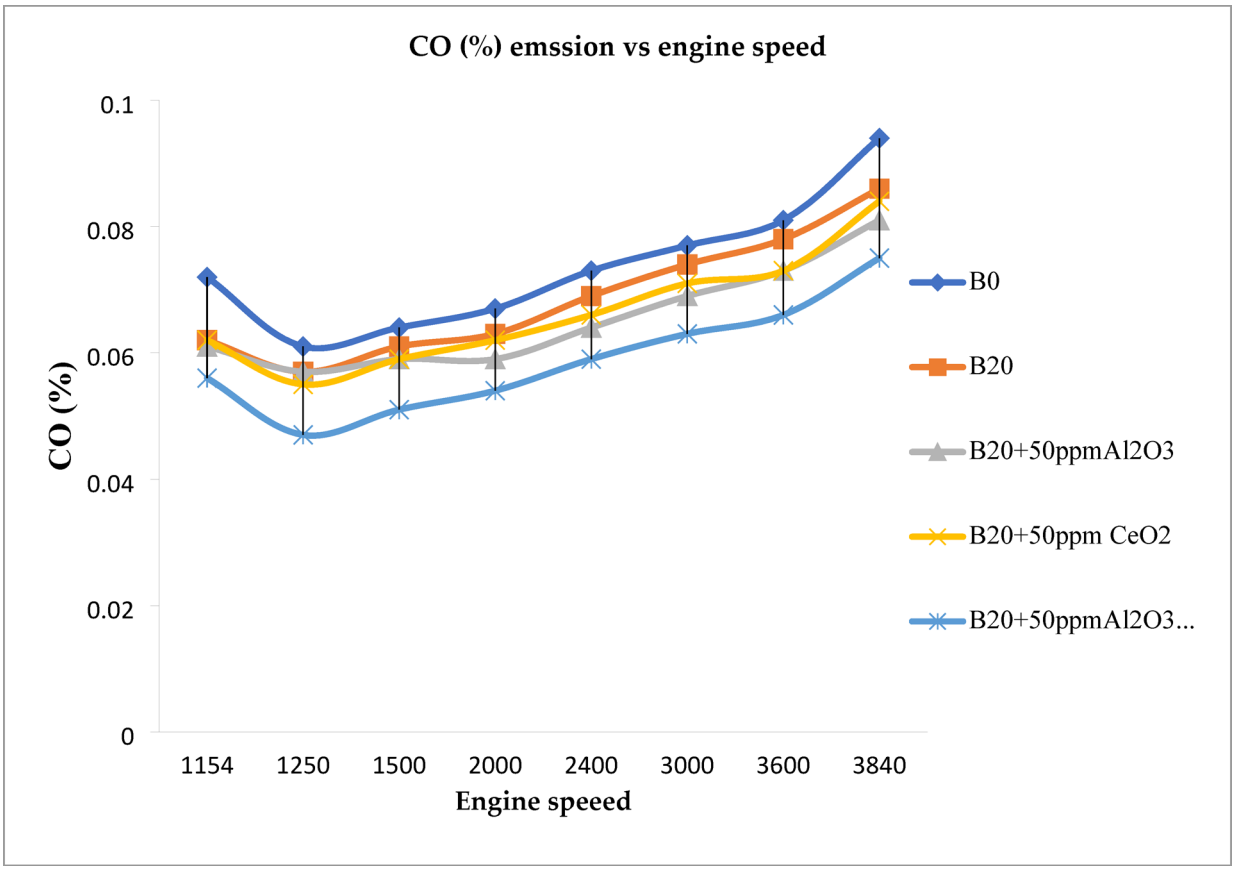

Fig. 13. Carbon monoxide (CO) emissions at different engine speeds.

Oxygen (O_2) emission

The oxygen (O_2) concentration in the exhaust gases was consistently higher for all biodiesel blends compared to conventional diesel (B0). This increase is primarily due to the inherent oxygen content of biodiesel fuels and is further enhanced by the catalytic effects of Al_2O_3 and CeO_2 nanoparticles, rather than being indicative of incomplete combustion. At 1554 rpm, the measured O_2 concentrations were 16.51% for B0, 17.63% for B20, 17.74% for B20 + 50 ppm Al_2O_3, 17.83% for B20 + 50 ppm CeO_2, and 17.97% for the B20 blend containing a combination of 50 ppm Al_2O_3 and 50 ppm CeO_2, as illustrated in Fig. 16. The elevated O_2 levels observed in the biodiesel and nanoparticle-enhanced blends reflect the additional oxygen supplied by the fuel molecules and the improved combustion environment created by the nanoparticles, which promote more complete and efficient oxidation of the fuel. Overall, these results indicate that the higher exhaust oxygen content is a beneficial effect of biodiesel and nanoparticle additives, supporting enhanced combustion processes rather than signaling any decrease in engine efficiency.

Comparison of the current study with recent work

This study was compared with previous literature based on the type of biodiesel used, engine operating conditions (speed and load), the nanoparticles or additives applied, and the resulting performance and emission outcomes. The comparison is summarized in Table 4.

Conclusion

This study investigated the effects of cottonseed biodiesel (B20) and its blends with aluminum oxide (Al_2O_3) and cerium oxide (CeO_2) nanoparticles on the performance and emissions of a single-cylinder CI engine. The brake power of diesel (B0) was 3.02 kW, while B20 alone produced 2.89 kW. Adding nanoparticles improved performance: B20 + 50 ppm Al_2O_3 reached 3.21 kW, B20 + 50 ppm CeO_2 reached 3.35 kW, and the combined B20 + 50 ppm Al_2O_3 + 50 ppm CeO_2 achieved the highest brake power of 3.56 kW. For brake torque, B0 recorded 8.5 Nm, B20 produced 8.1 Nm, and the nanoparticle blends improved it to 8.2 Nm with Al_2O_3, 8.4 Nm with CeO_2, and 8.6 Nm with the combined blend. The brake specific fuel consumption (BSFC) was highest for B20 due to its lower energy content, while the combined nanoparticle blend had the lowest BSFC of 0.258 kg/kW.h, showing better fuel efficiency.

All biodiesel blends reduced emissions compared to diesel. The combined B20 + Al_2O_3 + CeO_2 blend achieved the largest reductions: 23.2% in CO, 14.8% in CO_2, and 18.5% in HC, while also increasing exhaust oxygen levels to 17.97%, indicating more complete combustion. These improvements are due to the multifunctional

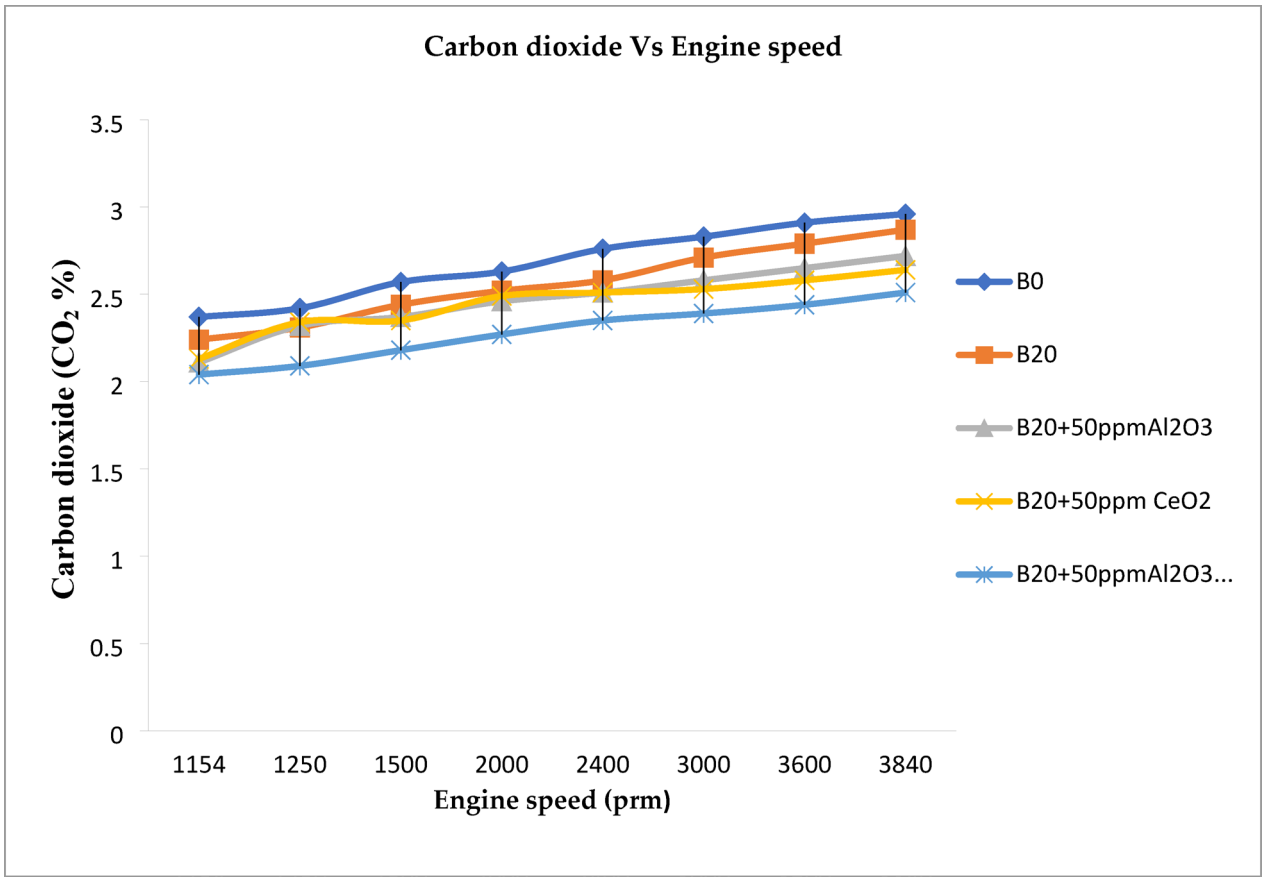

Fig. 14. Variation of Carbon dioxide (CO_2) emissions with engine speed.

role of the nanoparticles: they act as catalysts to enhance fuel oxidation, improve fuel atomization and air–fuel mixing, accelerate flame propagation, and, in the case of CeO_2, supply extra oxygen during combustion. Overall, adding Al_2O_3 and CeO_2 nanoparticles significantly enhances the performance and emission characteristics of B20 biodiesel without any engine modifications, offering a cleaner and more efficient fuel option.

Future work

This study has two main limitations: it was conducted on a single-cylinder research engine, and NOx emissions were not measured, which may affect the assessment of emission trade-offs. Future research should address these limitations.

Scalability

The findings should be validated on multi-cylinder diesel engines under realistic operating conditions to evaluate scalability, performance, and durability in real-world applications.

NOx reduction

Further studies should focus on optimizing the type and dosage of nanoparticles and investigating their combined effect with techniques such as exhaust gas recirculation (EGR) to specifically reduce NOx emissions from biodiesel–diesel blends.

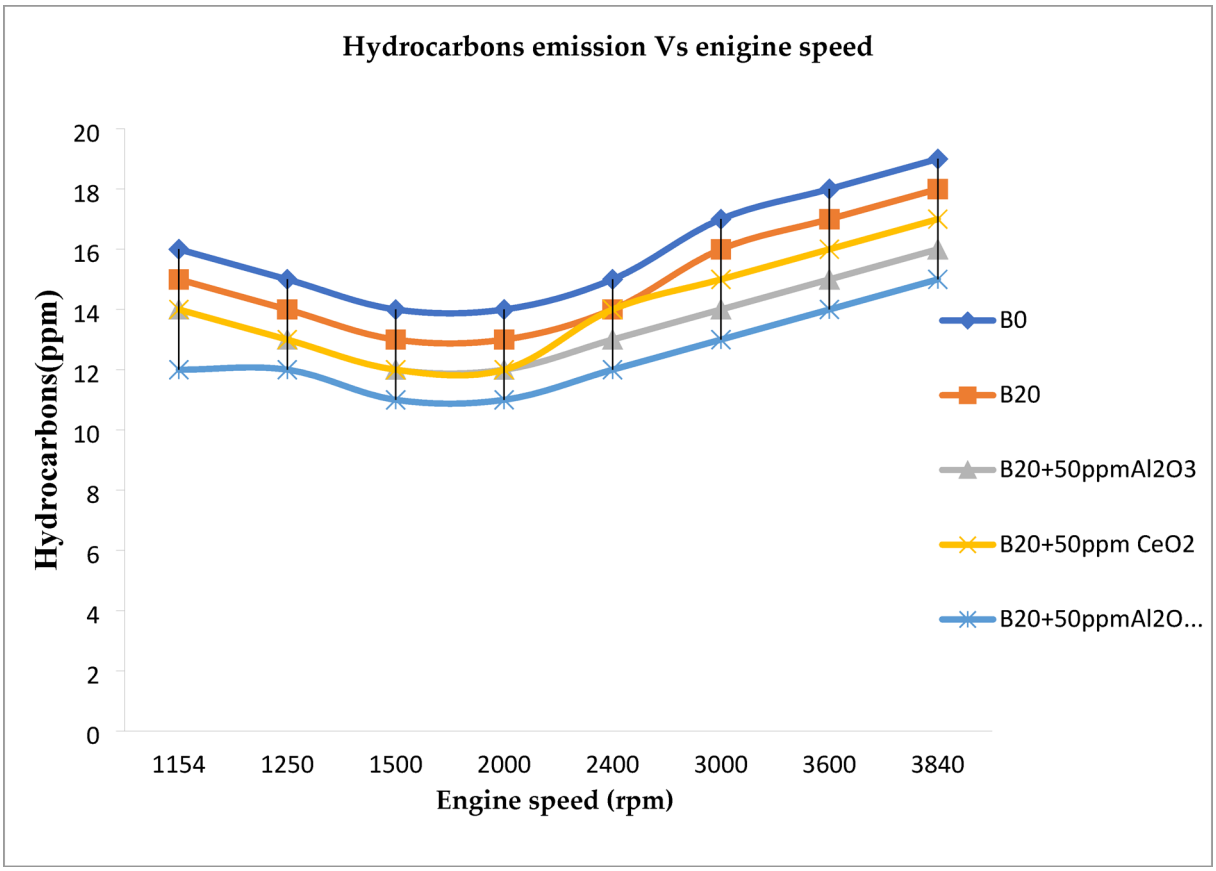

Fig. 15. Variation of hydrocarbon emissions with engine speed.

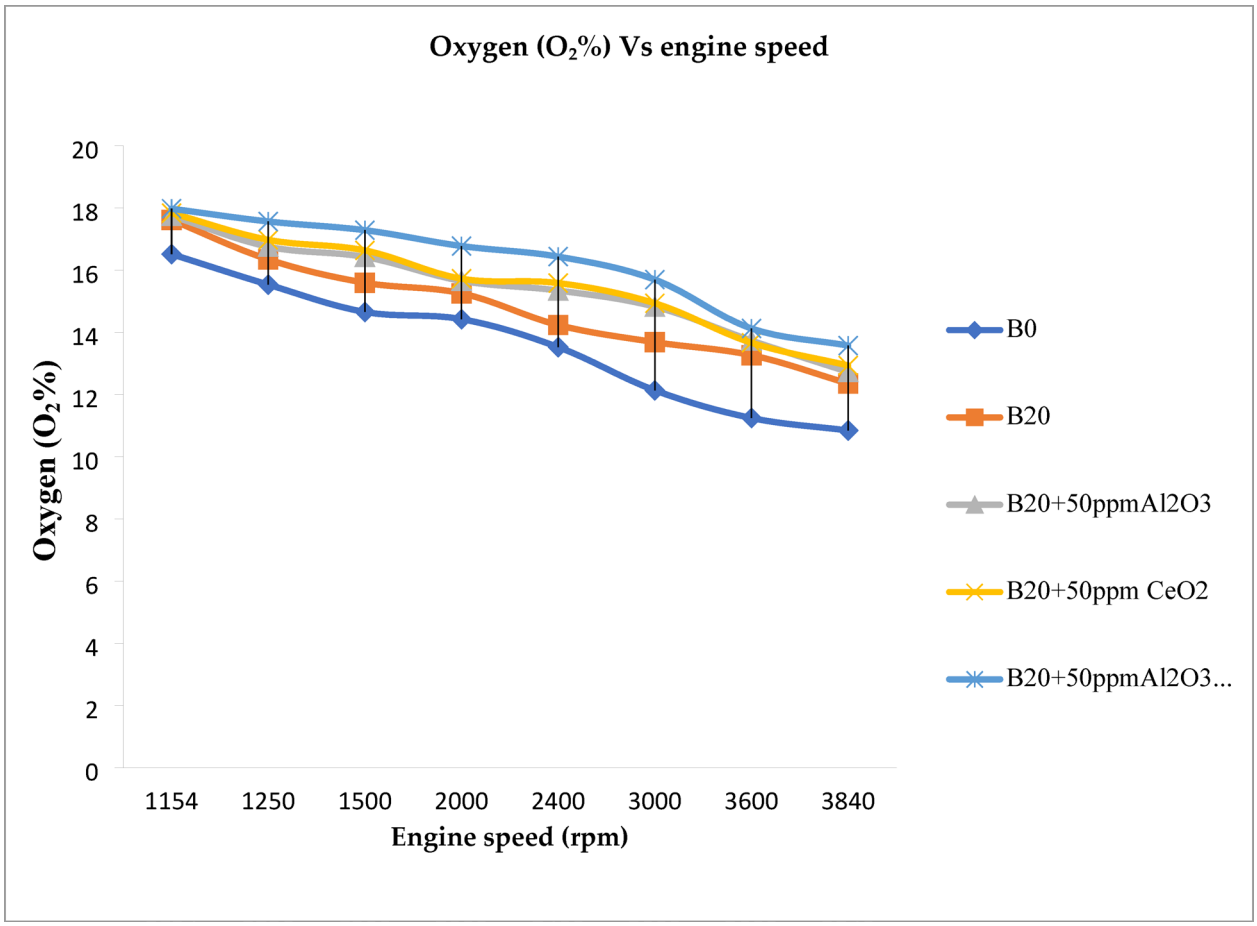

Fig. 16. Variation of oxygen (O_2) with engine speed.

Ref	Oil/biodiesel	Engine speed & load	Nanoparticles	Emissions and performance
[51]	WCO	1500 rpm	CeO_2 80 ppm	BSFC and NOx were reduced by 2.5% and 15.7%, respectively
[60]	CSME	0%–100% engine load	ZnO 40,80,120 ppm	At 80 ppm minimum, NOx and BSFC were obtained with better BTE
[61]	Jatropha biodiesel	80% load and 1700–2900 rpm	Al_2O_3 100 ppm	Maximum Tb and Pb were recorded with high NOx at engine speed of 2400–2600 rpm
[62]	Mahua	80% engine load	CuO 25, 50, 75 ppm	4.6% HC, 15.725% CO, with less BSFC were obtained at M20NP50
[63]	Jatropha biodiesel	Not specified	CeO_2 and Al_2O_3 at 10,30,60 ppm	13% NOx, 60% CO, and 32% of emission reduction were observed at 30A30C
[64]	Jatropha biodiesel	2600, 2900, 3200, 3500 rpm	Graphene oxide	Tb, HC, and CO_2 were improved in the finds, and Pb was reduced by 6.3%
[65]	B20 CSOME/Diesel	Not specified	100 ppm CeO_2	Reported a 23% reduction in CO and an 8% increase in Brake Thermal Efficiency (BTE). A significant increase in NOx emissions was noted as a drawback of the single additive
[66]	B20 Cottonseed	Not specified	75 ppm Al_2O_3	Reported a 9.2% increase in Brake Power (BP) and a 35% reduction in NOx. The study noted poorer performance in controlling CO and HC emissions
Present study	B20 fuel (20% cottonseed biodiesel, 80% diesel)	1154, 1250, 1500, 2000, 2400,3000, 3600, and 3840 rpm engine speed	Al_2O_3 50 ppm, CeO_2 50 ppm, $Al_2O_3 + CeO_2$ 50 + 50 ppm	B20 with 50 ppm Al_2O_3 and 50 ppm CeO_2 increased brake power by 17.9% (vs. 6.3% Al_2O_3, 4.3% CeO_2), achieved the highest brake torque, improved BSFC over B20, and reduced emissions: CO by 23.2%, CO_2 by 14.8%, and HC compared to diesel

Table 4. Critical summary of recent literature on nano-enhanced biodiesel.

Data availability

The corresponding author can provide the data used in this work upon reasonable request.

Received: 25 September 2025; Accepted: 30 October 2025
Published online: 28 November 2025

References

1. Yılbaşı, Z. Biofuels, E-fuels, and waste-derived fuels: advances, challenges, and future directions. *Sustainability* **17**(13), 6145 (2025).

2. V. Thanigaivelan and M. Loganathan, Investigational analysis of performance characteristics and emission of cashew nut shell biodiesel on DI diesel engine. *Int. J. Adv. Res. Eng. Technol.* vol. 10, no. 1, 2019.
3. Piri, H., Renzi, M. & Bietresato, M. Technical implications of the use of biofuels in agricultural and industrial compression-ignition engines with a special focus on the interactions with (bio) lubricants. *Energies* **17**(1), 129 (2023).
4. Mishra, V. K. & Goswami, R. A review of production, properties and advantages of biodiesel. *Biofuels* **9**(2), 273–289 (2018).
5. Linganiso, E. C. et al. Biodiesel production from waste oils: A South African outlook. *Sustainability* **14**(4), 1983 (2022).
6. Tulashie, S. K. et al. A review on the production of biodiesel from waste cooking oil: A circular economy approach. *Biofuels* **16**(1), 99–119 (2025).
7. Leng, L., Li, W., Li, H., Jiang, S. & Zhou, W. Cold flow properties of biodiesel and the improvement methods: A review. *Energy Fuels* **34**(9), 10364–10383 (2020).
8. Mohan, C. & Robinson, J. 11 Life cycle analysis of bio-based lubricants, *Biolubricants: Feedstocks. Catalysts Nanotechnol.* **1**, 185 (2024).
9. Tucki, K. et al. Estimation of carbon dioxide emissions from a diesel engine powered by lignocellulose derived fuel for better management of fuel production. *Energies* **13**(3), 561 (2020).
10. Douvartzides, S. L., Charisiou, N. D., Papageridis, K. N. & Goula, M. A. Green diesel: Biomass feedstocks, production technologies, catalytic research, fuel properties and performance in compression ignition internal combustion engines. *Energies* **12**(5), 809 (2019).
11. C. Vijai, D. Babu, N. Babu, and H. Alemayehu, "Optimizing Combustion Efficiency and Emission Reduction in Low Temperature Combustion Engines Using Biodiesel-Nano Additive Alcohol Blends: A Review," *Results in Engineering,* p. 106175, 2025.
12. Patel, A., Agrawal, B. & Rawal, B. Assessment of diesel engine performance and emission using biodiesel obtained from eucalyptus leaves. *Eur. J. Sustain. Dev. Res* **7**, 1–13 (2023).
13. M. Naeem, M. Imran, S. Latif, and N. Hussain, "Cerium-and aluminum-based nanomaterials as additive in nanofuels," In *Nanotechnology for Advanced Biofuels*: Elsevier, 2023, pp. 1–16.
14. Ghazaly, N. M. & Abdulhameed, A. N. Performance and emissions of nanoadditives in diesel engine: A. *Jurnal Ilmiah Teknik Elektro Komputer dan Informatika (JITEKI)* **9**(4), 997–1008 (2023).
15. Ahmed, M. M., Pali, H. S. & Khan, M. M. Feasibility of nanoparticles fused in biodiesel for CI engines: An integrated and historic review. *J. Therm. Anal. Calorim.* **149**(11), 5091–5123 (2024).
16. Lv, J., Wang, S. & Meng, B. The effects of nano-additives added to diesel-biodiesel fuel blends on combustion and emission characteristics of diesel engine: A review. *Energies* **15**(3), 1032 (2022).
17. Subramani, K. & Karuppusamy, M. Performance, combustion and emission characteristics of variable compression ratio engine using waste cooking oil biodiesel with added nanoparticles and diesel blends. *Environ. Sci. Pollut. Res.* **28**(45), 63706–63722 (2021).
18. Dhaka, A., Mali, S. C., Sharma, S. & Trivedi, R. A review on biological synthesis of silver nanoparticles and their potential applications. *Results Chem.* **6**, 101108 (2023).
19. Mofijur, M. et al. Impact of nanoparticle-based fuel additives on biodiesel combustion: An analysis of fuel properties, engine performance, emissions, and combustion characteristics. *Energy Convers. Manag. X* **21**, 100515 (2024).
20. Gowthaman, S. & Thangavel, K. Performance, emission and combustion characteristics of a diesel engine fuelled with diesel/coconut shell oil blends. *Fuel* **322**, 124293 (2022).
21. Elkelawy, M. et al. Enhancing CI engine performance and emissions through PCCI and sustainable combustion solutions with waste cooking oil biodiesel blends a comparative study. *Sci. Rep.* **15**(1), 24617 (2025).
22. Ninawe, G. A comprehensive review of engine performance enhanced by nano additives infused within a diesel-biodiesel blend for internal combustion engines. *Int. J. Veh. Perform.* **11**(2), 159–189 (2025).
23. Pullagura, G. et al. Effect of nano additives on fuel properties, engine performance, emission and combustion characteristics of CI engines fuelled with diesel and biodiesel blends: A comprehensive review. *Bull. Monum.* **21**(11), 39–50 (2021).
24. Basha, J. S. et al. Applications of nano-additives in internal combustion engines: A critical review. *J. Therm. Anal. Calorim.* **147**(17), 9383–9403 (2022).
25. Vijayakumar, C. et al. Biodiesel from plant seed oils as an alternate fuel for compression ignition engines—A review. *Environ. Sci. Pollut. Res.* **23**(24), 24711–24730 (2016).
26. D. Kumar, V. K. Chhibber, A. Singh, and A. Kumar, "Vegetable seed oils as biofuel: Need, motivation, and research identifications," *Clean Renew. Energy Prod.* pp. 1–25, 2024.
27. Baweja, S., Trehan, A. & Kumar, P. Experimental Investigation for Single Cylinder Engine Fueled with Mustard Oil Biodiesel. In *International Conference on Humainzing Work and Work Environement* 221–241 (Springer, 2019).
28. Mazari, F. A study on emission reduction and combustion efficiency, analyzing oxymethylene ether (OME1-5) with diesel fuel. *Fuel* **375**, 132578 (2024).
29. Tomar, M. & Kumar, N. Influence of nanoadditives on the performance and emission characteristics of a CI engine fuelled with diesel, biodiesel, and blends—A review. *Energy Sourc. Part A Recov. Util. Environ. Eff.* **42**(23), 2944–2961 (2020).
30. J. R. Bikkavolu *et al.*, "Employing hydrogen infusion to improve the combustion attributes of Di-methyl carbonate-boron nitride-biodiesel/diesel blends in a diesel engine," *Int. J. Hydrog. Energy,* 2024.
31. J. R. Bikkavolu, R. K. Tota, K. R. Chebattina, L. R. Bhagavatula, G. Pullagura, and P. Seepana, "Predicting Common Rail Direct Injection (CRDI) engine metrics using nanoparticle-enhanced pongamia pinnata biodiesel with machine learning," *Emerg. Mater.* pp. 1–18, 2025.
32. Navas, M. B., Lick, I. D., Bolla, P. A., Casella, M. L. & Ruggera, J. F. Transesterification of soybean and castor oil with methanol and butanol using heterogeneous basic catalysts to obtain biodiesel. *Chem. Eng. Sci.* **187**, 444–454 (2018).
33. Nayab, R. et al. Sustainable biodiesel production via catalytic and non-catalytic transesterification of feedstock materials–A review. *Fuel* **328**, 125254 (2022).
34. Mandari, V. & Devarai, S. K. Biodiesel production using homogeneous, heterogeneous, and enzyme catalysts via transesterification and esterification reactions: A critical review. *BioEnergy Res.* **15**(2), 935–961 (2022).
35. Sambandam, P. et al. Investigation of the environmental implications of using cerium oxide nano-additives in gasoline engines fueled with gasoline-oxyhydrogen. *Energy Sour. Part A Recov. Util. Environ. Eff.* **46**(1), 11584–11603 (2024).
36. Mostafa, A., Mourad, M., Mustafa, A. & Youssef, I. Influence of aluminum oxide nanoparticles addition with diesel fuel on emissions and performance of engine generator set using response surface methodology. *Energy Convers. Manag. X* **19**, 100389 (2023).
37. Sujesh, G., Ganesan, S. & Ramesh, S. Effect of CeO2 nano powder as additive in WME-TPO blend to control toxic emissions from a light-duty diesel engine–An experimental study. *Fuel* **278**, 118177 (2020).
38. Chetia, B., Debbarma, S. & Das, B. Enhancing engine performance, combustion, and emissions characteristics through CeO2-modified cottonseed biodiesel with hydrogen enrichment: A comprehensive investigation. *Int. J. Hydrog. Energy* **89**, 1149–1165 (2024).
39. J. Ampah *et al.*, "Progress and Recent Trends in the Application of Nanoparticles as Low Carbon Fuel Additives—A State of the Art Review. Nanomaterials 2022; 12: 1515," ed: s Note: MDPI stays neutral with regard to jurisdictional claims in published, 2022.
40. Ronaghi, T. B., Fotovat, F. & Zamzamian, S. A. H. Enhancing cerium oxide nanoparticle stability in diesel–biodiesel blends via alumina nanoparticle amalgamation. *Waste Biomass Valoriz.* **15**(11), 6107–6120 (2024).
41. Fatimah, I., Nugraha, J., Sagadevan, S., Kamari, A. & Oh, W.-C. Process intensification of biodiesel production by optimization using box-behnken design: A review. *Chem. Eng. Process. Process Intensif.* **208**, 110110 (2025).

42. Tefera, N. T., Nallamothu, R. B., Alemayehu, G. & Kefale, Y. Optimization, characterization, and GC-MS analysis of CSOME produced using alkali catalyzed transesterification. *Energy Convers. Manag. X* **22**, 100549 (2024).
43. J. K. Satyarthi, Catalytic conversion of vegetable oils to biofuels over transition metal catalysts, 2011.
44. Gashaw, A. & Lakachew, A. Production of biodiesel from non edible oil and its properties. *Int. J. Sci. Environ. Technol.* **3**(4), 1544–1562 (2014).
45. Estevez, R. et al. Biodiesel at the crossroads: A critical review. *Catalysts* **9**(12), 1033 (2019).
46. N. S. Caetano, V. Ribeiro, L. Ribeiro, A. Baptista, and J. Monteiro, "Biodiesel production systems: operation, process control and troubleshooting," In *Biodiesel: from production to combustion*: Springer, 2018, pp. 27–56.
47. Berrios, M., Martín, M., Chica, A. & Martín, A. Purification of biodiesel from used cooking oils. *Appl. Energy* **88**(11), 3625–3631 (2011).
48. Alves, A. A. et al. Distillation analysis of diesel-biodiesel mixtures: A comparative study with ASTM norms, experimental data, and novel correlations. *Fuel* **383**, 133864 (2025).
49. Ong'era, C., Gathitu, B., Murunga, S., Kuloba, P. & Gathirwa, J. Evaluation of flash point and calorific value of nanostructured rapeseed oil biodiesel as an automotive fuel. *J. Agric. Sci. Technol.* **23**(1), 115–124 (2024).
50. Hameed, A. Z. & Muralidharan, K. Performance, emission, and catalytic activity analysis of AL2O3 and CEO2 nano-additives on diesel engines using mahua biofuel for a sustainable environment. *ACS Omega* **8**(6), 5692–5701 (2023).
51. Dinesha, P., Kumar, S. & Rosen, M. A. Effects of particle size of cerium oxide nanoparticles on the combustion behavior and exhaust emissions of a diesel engine powered by biodiesel/diesel blend. *Biofuel Res. J.* **8**(2), 1374–1383 (2021).
52. M. M. Abbas, "Comparative Study of Nanoparticles and Alcoholic Fuel Additives with Optimized Synthesis of Palm-sesame Biodiesel Using Tribological and Internal Combustion Engine Testing," University of Malaya (Malaysia), 2021.
53. S. Khalighi, "Biodiesel production: determination of thermodynamic properties and monitoring of the transesterification reaction," Universidade de Coimbra, 2024.
54. S. K. Kuppili, A. Kumar, and D.-S. Kim, Biodiesel Properties Depending on Blends and Feedstocks: 155Cloud Point, Kinematic Viscosity, and Flash Point, In *World Biodiesel Policies and Production*: CRC Press, 2019, pp. 155–174.
55. Mengistu, N. G., Mekonen, M. W., Ayalew, Y. G., Demisie, L. F. & Nega, T. Experimental investigation on diesel engine performance and emission characteristics using waste cooking oil blended with diesel as biodiesel fuel. *Discov. Energy* **4**(1), 26 (2024).
56. Sathish, T., Giri, J., Saravanan, R., Zairov, R. & Hasnain, S. M. Nano-fuels of Al2O3/SiO2/MgO/tamarind seed oil biodiesel for CI engines: An evaluation of combustion consumption and emission performance. *Int. J. Thermofluids* **23**, 100815 (2024).
57. Posada-Pérez, S., Solà, M. & Poater, A. Carbon dioxide conversion on supported metal nanoparticles: A brief review. *Catalysts* **13**(2), 305 (2023).
58. Patnaik, D., Pattanaik, A. K., Bagal, D. K. & Rath, A. Reducing CO2 emissions in the iron industry with green hydrogen. *Int. J. Hydrogen Energy* **48**(61), 23449–23458 (2023).
59. A. A. Yusuf, F. L. Inambao, and J. D. Ampah, "The effect of biodiesel and CeO2 nanoparticle blends on the CRDI diesel engine: A special focus on combustion, particle number, PM2. 5 species, organic compound, and gaseous emissions," *Journal of King Saud University-Engineering Sciences*, 2022.
60. Kumar, T. D., Hussain, S. S. & Ramesha, D. Effect of a zinc oxide nanoparticle fuel additive on the performance and emission characteristics of a CI engine fuelled with cotton seed biodiesel blends. *Mater. Today Proc.* **26**, 2374–2378 (2020).
61. Teklehaimanot, H., Gupta, N. & Nallamothu, R. B. The impact of Al2O3 nano additives on Jatropha curcas biodiesel-diesel blend on combustion and emission behavior. *Energy Convers. Manag. X* **25**, 100870 (2025).
62. Muniyappan, S. & Krishnaiah, R. Investigation on CuO nanoparticle enhanced mahua biodiesel/diesel fuelled CI engine combustion for improved performance and emission abetted by response surface methodology. *Sci. Rep.* **14**(1), 26882 (2024).
63. Prabu, A. & Anand, R. Emission control strategy by adding alumina and cerium oxide nano particle in biodiesel. *J. Energy Inst.* **89**(3), 366–372 (2016).
64. Hammad, S. M. et al. Enhancing diesel engine performance and emissions control with reduced graphene oxide and non-edible biodiesel blends. *Energy Convers. Manag. X* **24**, 100710 (2024).
65. Tamrat, S., Ancha, V. R., Gopal, R., Nallamothu, R. B. & Seifu, Y. Emission and performance analysis of diesel engine running with CeO_2 nanoparticle additive blended into castor oil biodiesel as a substitute fuel. *Sci. Rep.* **14**(1), 7634 (2024).
66. G. P. K. Yadav, P. Muvvala, and R. M. Reddy, Optimization of injection parameters, and ethanol shares for cottonseed biodiesel fuel in diesel engine utilizing artificial neural network (ANN) and taguchi grey relation analysis (GRA)., *J. Non Equilib. Thermodyn.*, 2025.

Author contributions

Debas Dessie, Eyob Sisay Yeshanew: Conceptualization, Methodology, Experimental Testing, Validation, Systematic Analysis, Experimental Investigation, Data Processing, and Preparation of the Original Research Document. Ramesh Babu Nallamothu, Getachew Gashaw: Conceptualisation, Methodology, Validation, Writing-Reviewing and Editing.

Declarations

Competing interests

The authors declare no competing interests.

Additional information

Correspondence and requests for materials should be addressed to E.S.Y.

Reprints and permissions information is available at www.nature.com/reprints.

Publisher's note Springer Nature remains neutral with regard to jurisdictional claims in published maps and institutional affiliations.